



Symmetrical tilt grain boundaries in bcc transition metals: comparison of semiempirical with *ab-initio* total-energy calculations

T. OCHS, C. ELSÄSSER†

Max-Planck-Institut für Metallforschung, Seestraße 92, D-70174 Stuttgart, Germany

M. MROVEC, V. VITEK

Department of Materials Science and Engineering, University of Pennsylvania, Philadelphia, Pennsylvania 19104-6272, USA

J. BELAK and J. A. MORIARTY

Lawrence Livermore National Laboratory, Physics Directorate, POB 808, Livermore, California 94550, USA

[Received 24 August 1999 and accepted in revised form 25 November 1999]

ABSTRACT

Five different semiempirical total-energy methods, provided in the literature and applicable for atomistic simulations of extended defects in bcc transition metals, are investigated in a comparative study. The comparison is made with recent theoretical *ab-initio* (local-density-functional theory) and experimental (high-resolution transmission electron microscopy) studies for the specific case of the $\Sigma = 5$, (310)[001] symmetrical tilt grain boundaries ($\Sigma = 5$ STGBs) in Nb and Mo. The considered semiempirical real-space approaches based on different approximations of the tight-binding and related methods are the Finnis–Sinclair central-force potentials, non-central-force bond-order potentials recently advanced by Pettifor and co-workers, and non-central-force potentials based on the model-generalized pseudopotential theory of Moriarty. As semiempirical reciprocal-space methods, a very simple d-basis tight-binding model by Paxton and an elaborate environment dependent spd-basis orthogonal tight-binding model by Haas *et al.* are included in the analysis. The virtues and deficiencies of these models in their ability to predict the translation states and interfacial energies of the $\Sigma = 5$ STGB are discussed.

§1. INTRODUCTION

Atomistic simulations of the structures and physical properties of extended crystal defects, such as dislocations, interfaces and surfaces, have now become a very important area of materials research (Mark *et al.* 1992, Broughton *et al.* 1993, Phillpot *et al.* 1998, Turchi *et al.* 1998). The essential precursor of such studies is a description of interatomic interactions or, more generally, a knowledge of the dependence of the total energy on the relative positions of the atoms in the studied

† Email: elsae@marvin.mpi-stuttgart.mpg.de.

system. In principle, this is provided very accurately by *ab-initio* total-energy calculations based on the local-density functional theory (LDFT) (Hohenberg and Kohn 1964, Kohn and Sham 1965) that have been utilized extensively in recent years in studies of crystalline materials. However, in such calculations the required computational effort is very high and they are normally only feasible when the number of atoms included in the calculation is not much more than 100. This is totally inadequate for the majority of extended defects. The most obvious cases are dislocations that are associated with long-range elastic fields. However, even in the case of interfaces and surfaces, only very special short-period structures can be studied adequately with such numbers of atoms. Hence, the bulk of the modelling of extended defects has been made using much simpler approaches (for overviews see Vitek (1994) and Voter (1996)).

In recent years the many-body central-force potentials of the embedded-atom method (EAM) (Daw and Baskes 1984, Daw *et al.* 1993, Foiles 1996) and the Finnis–Sinclair (FS) type (Finnis and Sinclair 1984, 1986, Ackland *et al.* 1987, 1988), were very successful in studies of metallic materials, in particular noble metals and their alloys as well as Ni and Ni–Al alloys (for example Ackland *et al.* (1987), Ackland and Vitek (1990), Daw *et al.* (1993), Ludwig and Gumbsch (1995) and Yan *et al.* (1996)). In these semiempirical schemes the total energy is only a function of separations of atomic pairs and any possible directional character of bonding is excluded but, contrary to the pair potentials, the cohesive part of the total energy has a many-body character (for example Ackland *et al.* (1988) and Foiles (1996)). This approach was also applied to bcc and hcp transition metals (Finnis and Sinclair 1984, 1986, Ackland and Thetford 1987, Ackland 1992) but in several cases it was found inadequate, presumably because the angular component of the bonding in these metals is significant. This is not surprising since it is well known that in transition metals the relative stability of alternate crystal structures is controlled by the level of the filling of the d band (Friedel 1969, Pettifor 1995), and the bonding mediated by the d electrons has a covalent character. Consequently, it can be expected that the covalent component of bonding may also play a significant role in the determination of low-energy structures of extended lattice defects.

One of the first such tests was a calculation of the structure of the $\Sigma = 5$, (310)[001] symmetrical tilt grain boundary ($\Sigma = 5$ STGB) in Nb that was linked with high-resolution transmission electron microscopy (HRTEM) (Campbell *et al.* 1992, 1993). The calculation using central-force potentials resulted in the low-energy structure with a relative displacement of grains in the [001] direction, while HRTEM observations revealed a structure with mirror symmetry of the bicrystal and thus no lateral relative displacement of the grains. In the same study it was shown that the mirror symmetry was reproduced when non-central-force potentials based on the model-generalized-pseudopotential theory (MGPT) (Moriarty 1990, 1994) were employed. An analogous but opposite discrepancy appeared recently for the case of the $\Sigma = 5$ STGB of Mo. Bacia *et al.* (1997) obtained a mirror-symmetrical grain-boundary configuration for Mo by means of atomistic simulations with a central-force *n*-body cohesion model, which was based on the second-moment tight-binding approximation like the FS potentials. This result turns out to be in contradiction with a very recent experimental HRTEM observation of Campbell *et al.* (1999). Similar inadequacies were also found in atomistic simulations of surfaces (Carlsson 1991, Foiles 1993) and studies of dislocations in Ti. In the latter case, central forces predict incorrectly the basal plane as the slip plane while bond-order

potentials (BOPs) (Pettifor 1989, Aoki 1993, Horsfield *et al.* 1996a,b, 1998, Bowler *et al.* 1997) that include directional bonding predict correctly the prism plane as the slip plane (Girshick *et al.* 1998a,b). Legrand (1984) has shown earlier that the controlling factor here is the electronic structure. Such inadequacies should not arise, of course, in *ab-initio* calculations but, as already discussed, these are not feasible for a broad variety of extended defects. On the other hand, the semiempirical methods that include directional bonding, most of which are based on the tight-binding approximation (for example Harrison (1980, 1994)), all contain approximations and their ubiquitous transferability to any complex structure is always debatable.

In this paper we investigate, as a case study, the above-mentioned $\Sigma = 5$ STGBs in Nb and Mo. The recent HRTEM observations for Mo suggest that, unlike for Nb, the minimum-energy structure does not possess mirror symmetry and the grains are relatively displaced in the [001] direction (Campbell *et al.* 1999). Furthermore, the recent *ab-initio* calculations employing the LDFT mixed-basis pseudopotential (MBPP) method (Elsässer *et al.* 1990, Ho *et al.* 1992, Meyer *et al.* 1998) clearly demonstrated that the $\Sigma = 5$ STGBs have different structures in Nb and in Mo respectively, with the translation states in agreement with HRTEM observations (Elsässer *et al.* 1998, Ochs *et al.* 2000). The scope and goal of the present work are to use the atomistic study of this boundary as a representative benchmark for the judgement of the capabilities of several existing semiempirical models describing interatomic interactions at defects in Nb and Mo. The models considered are adopted from studies reported in the literature in which they were tested by investigating a wide range of crystalline bulk and defect properties. They are the FS-type potentials constructed by Ackland and Thetford (1987), three different tight-binding methods and non-central MGPT potentials. All of them have been developed on the basis of physical understanding of the electronic structure and bonding in transition metals. Calculations for the same set of geometric grain-boundary configurations are always made by all these semiempirical methods and compared in detail with *ab-initio* calculations, in order to analyse the ability of the different semiempirical schemes to represent the essential features of interatomic bonding in the transition metals studied.

§2. COMPUTATIONAL APPROACHES

The *ab-initio* total-energy calculations that serve as a benchmark for the semiempirical models of the description of interatomic interactions were made using a MBPP electronic-structure technique (Louie *et al.* 1979, Fu and Ho 1983, Elsässer *et al.* 1990, Ho *et al.* 1992, Meyer *et al.* 1998). This method is based on the LDFT (Hohenberg and Kohn 1964, Kohn and Sham 1965) and can be used to evaluate total energies as well as atomic forces acting on individual atoms for any assembly of atoms in crystalline materials. The results of such *ab-initio* calculations for the $\Sigma = 5$ STGBs in Nb and Mo have recently been reported in detail (Elsässer *et al.* 1998, Ochs *et al.* 2000), and they are reproduced here for direct comparison with results obtained with semiempirical methods. All important computational details are summarized in the two above-mentioned papers.

Several material-specific semiempirical models for the description of interatomic interactions in Nb and Mo were investigated in this work. Formally four of them (FS, BOP, d tight-binding (d-TB) and spd orthogonal tight-binding (spd-OTB) models) can be derived from the first-principles LDFT by successive approximations for tightly bound electron states (tight-binding theory) and by empirical parametrization

of functional dependences of individual contributions to the total energies on interatomic distances and angles. The fifth (MGPT) is obtained by systematic approximation and parametrization of the first-principles LDFT-based generalized pseudopotential theory (GPT) (Moriarty 1988) in a hybrid representation of tight-binding and nearly-free-electron models.

Total energies are composed of several contributions determined explicitly by the electronic structure. The first, attractive contribution, is the 'band energy' in tight-binding band models (Harrison 1980, 1994) or the 'bond energy' in tight-binding bond models (Sutton *et al.* 1988; Pettifor 1995). This contribution, usually evaluated in the two-centre approximation for the interatomic matrix elements (hopping integrals), reflects the angular dependence of the energy that enters via the angular character of these two-centre integrals (Slater and Koster 1954). The second contribution is repulsive and arises from the electrostatic double-counting and other many-body contributions not included in the band or bond parts of the total energy. This contribution is of short range and is usually described by empirical central-force terms, most commonly by pair potentials, although BOP and spd-OTB include repulsive environment-dependent terms. The parameters entering these schemes are determined by fitting to some specific properties of a material considered. For the schemes employed in this study they either are available in the literature (Finnis and Sinclair 1984, 1986, Ackland and Thetford 1987, Paxton 1996) or have been determined in studies preceding the present investigation (Haas *et al.* 1998a,b, Mrovec *et al.* 1999).

The models considered in the present work all utilize the orthogonal and two-centre tight-binding approximations (for example Harrison (1980)). However, they can be divided into two classes according to the approach to the evaluation of the band and/or bond energy. The first class employs the reciprocal-space Bloch representation of electrons in crystalline materials, and calculations require the use of three-dimensional periodic boundary conditions. Thus, supercells have to be used, similarly as in *ab-initio* calculations. The second class is formulated in a real-space electronic-structure representation and, therefore, periodic boundary conditions are not needed. This is very advantageous when studying extended crystal defects without periodicities in some spatial directions. Furthermore, it is equally applicable to crystalline and non-crystalline materials.

The first class of methods consists of the following two tight-binding band models. The model that treats only d orbitals explicitly in the tight-binding Hamiltonian (d-TB) includes no condition of self-consistency (such as local charge neutrality), and the repulsion is described by a pair potential (Spanjaard and Desjonquères 1984). It was parametrized and applied previously to a Nb $\Sigma = 5$ STGB by Paxton (1996). In the other model, developed by Haas *et al.* (1998a,b) for Mo and extended by Haas to Nb for the present study (H. Haas, personal communication), an orthogonal tight-binding Hamiltonian is represented by a minimal basis of s, p and d valence orbitals (spd-OTB). Furthermore, it accounts in an empirical fashion for an environment dependence of the on-site and the hopping matrix elements and a bond-length scaling depending on the local atomic coordination. The repulsion is represented by pairwise interactions which include an environment dependence in an analogous empirical manner to the hopping matrix elements. Self-consistency is not included in any way in this model. The parameters of this model were determined to reproduce linear muffin-tin orbital atomic-sphere approximation LDFT results for band structures and total energies (energy–volume curves) of bulk sc, bcc and fcc crystals,

and an additional set of experimental data or LDFT results outlined by Haas *et al.* (1998a, p. 1465) to improve the model concerning the phonon spectrum and properties of point defects and surfaces. The parameter-fitting strategy of this rather complex tight-binding model is explained in detail in the two papers by Haas *et al.* (1998a,b).

In the second class of methods, three models are considered. The first employs central-force many-body potentials developed originally by Finnis and Sinclair (1984, 1986) and Ackland and Thetford (1987). These interatomic potentials can be interpreted as a description of the total energy in the scalar second-moment approximation to the tight-binding electron density of states combined with the condition of orbital charge neutrality (Ackland *et al.* 1988). They can also be considered as a particular variant of the EAM (Daw and Baskes 1984, Daw *et al.* 1993). The parameters in these potentials were fitted to reproduce the equilibrium lattice constant, the cohesive energy, the elastic constants and, approximately, the vacancy formation energy. They account for the non-local character of the metallic bonding by combining a purely pairwise, mainly repulsive interatomic interaction with an electron-density-dependent functional. However, angle-dependent interactions occurring because of the partial filling of d bands in transition metals are neglected although these have been identified to be responsible for the preference of the Va and VIa transition metals to crystallize in the bcc structure instead of close-packed (fcc or hcp) structures (for example Pettifor (1995)).

Angle-dependent interactions can be included into semiempirical potentials based on tight-binding models by introducing matrix second moments and by going beyond the second-moment approximation. Examples are the fourth-moment tight-binding (4MTB) potentials developed by Carlsson (1991) or by Foiles (1993). The former potentials were used in a recent study of STGB in Mo by Marinopoulos *et al.* (1995). More sophisticated and presumably more accurate schemes are the BOPs (Pettifor 1989) that were developed as a real-space formulation of the tight-binding bond model (Pettifor 1989, Aoki 1993, Horsfield *et al.* 1996a,b, 1998, Bowler *et al.* 1997, Girshick *et al.* 1998a).

The bond part of the total energy is written as a product of the bond order and the tight-binding Hamiltonian. The matrix elements of the latter are adjusted through the bond length scaling so as to reproduce *ab-initio* data of the electronic structure and other results such as energy differences between alternate metastable structures; however, unlike in the spd-OTB model, the interatomic matrix elements are not environment dependent. The bond order, the physical meaning of which is the difference between the number of electrons in the bonding and antibonding states, is evaluated via Green's functions represented as continued fractions, using the recursion method that can be related directly to a moment expansion (Pettifor and Weaire 1985, Horsfield *et al.* 1996a,b). The central-force repulsive part of the energy consists of an environment-dependent many-body term and a pair-potential term. The former represents the overlap repulsion that arises from the valence s and p electrons. Its functional form has been determined by a detailed analysis of the electronic contribution to the Cauchy pressures (Nguyen-Manh *et al.* 1998) and it is fitted to reproduce the Cauchy pressures. The pair potential is then fitted to reproduce the remaining elastic constants, equilibrium lattice parameters and cohesive energy. Additionally, effects of self-consistency are accounted for by the requirement of local charge neutrality. In the particular BOP for Mo and Nb applied in the present work the continuous fraction expansion was limited to four recursion levels, that is up to eight moments of the density of states were included. The fitting

included, together with the physical quantities mentioned above, the *ab-initio* calculated differences between sc, bcc and fcc structures (Mrovec *et al.* 2000).

The last real-space method considered is the MGPT that earlier had predicted the mirror symmetry of the $\Sigma = 5$ STGB in Nb (Campbell *et al.* 1992, 1993). This is a model representation of the first-principles LDFT-based GPT (Moriarty 1988), which provides a rigorous expansion of the total energy of a transition metal in terms of multiple-ion interatomic potentials. The leading volume term and the two-, three- and four-ion potentials normally retained in this expansion for bcc metals are volume-dependent but structure-independent quantities and thus transferable to all bulk atomic configurations. The GPT yields explicit sp nearly-free-electron-like, dd tight-binding-like and sp-d hybridization contributions to the volume term and interatomic potentials, with the three- and four-ion angular-force potentials reflecting dd and sp-d contributions from partially filled d bands. The first-principles potentials are necessarily long-ranged, non-analytic and multidimensional functions that cannot be easily tabulated for application purposes. This has led to the development of the simplified MGPT for bcc metals (Moriarty 1990, 1994). In the MGPT, the multiple-ion potentials are systematically approximated to achieve short-ranged analytic forms, which can then be widely applied to static and dynamic simulations. Specifically, the following simplifying approximations are introduced.

- (i) sp-d hybridization contributions are retained only in the volume term.
- (ii) d-state non-orthogonality is folded entirely into the two-ion pair potential and contributes to an effective hard-core repulsive interaction.
- (iii) Canonical d bands are used to represent the remaining d-state matrix elements analytically.

The two-centre tight-binding-like hopping terms then have a characteristic r^{-p} radial dependence and a 6 : -4 : 1 ratio for the $m = 0, 1, 2$ components. For pure canonical d bands, $p = 5$, but a value $p = 4$ is usually used as a better way to describe the d bands of real bcc metals.

To compensate for the approximations introduced in the MGPT, a limited amount of parameterization is allowed in which the coefficients of the modelled potential terms are constrained by external experimental or *ab-initio* data. Useful MGPT potentials have been determined in this way over a wide range of volumes for Mo to study melting and the high-pressure phase diagram (Moriarty 1994). Here the only quantities fitted to external data were the ambient-pressure bcc bulk and elastic moduli, the vacancy formation energy and the zero-temperature equation of state. Recently, these same potentials have also been successfully applied to ambient-density studies of point defects and dislocations (Xu and Moriarty 1996, 1998) and preliminary calculations of the $\Sigma = 5$ STGB in Mo (Campbell *et al.* 1999). In the present work, the full volume dependence of the Mo total energy is considered and one small technical refinement to the potentials has been added in the form of an improved long-range cut-off scheme.

The Nb MGPT potentials used in the present work are the same first-generation potentials as used by Campbell *et al.* (1992, 1993) in their original grain-boundary studies. These potentials were determined only at ambient density; so all calculations here are limited to this density. In determining the Nb potentials, similar data were fitted as in the case of Mo, except that the observed anomalous elastic constant C_{44} was replaced by the corresponding zone-boundary phonon. In both Mo and Nb, only bcc properties have been used in constraining the MGPT potentials.

§ 3. SIMULATION CELLS AND BOUNDARY CONDITIONS

In atomistic simulations of grain boundaries that employ real-space methods for the evaluation of the total energy, two-dimensional periodic Born–von Kármán boundary conditions are conveniently employed parallel to the boundary plane but no periodicity is introduced in the perpendicular direction. Thus the block of atoms used in such calculations is usually constructed as follows. First, its structure is arranged as a bicrystal with the desired boundary, characterized by the misorientation of the adjoining crystals and inclination of the boundary plane. Its lateral extensions are confined to the repeat cell of the boundary plane. In both axial directions it is composed of two domains. The first consists of the regions adjacent to the boundary in which the atoms are fully relaxed. These areas are then bounded by regions of atoms that are fixed at the crystal lattice positions. However, the two grains may displace relative to each other rigidly in all directions so that relative displacement parallel to the boundary as well as expansion or contraction may occur (for example, Sutton and Balluffi (1995) and Vitek (1996)).

On the other hand, *ab-initio* calculations and tight-binding calculations that employ the reciprocal-space methods for evaluation of the total energy require periodic boundary conditions in all three directions. This implies that in the direction perpendicular to the boundary a periodic sequence of boundaries has to be introduced, and a supercell containing two equivalent grain boundaries represents then a three-dimensional repeat unit of this structure. In the previous *ab-initio* LDFT calculations and the reciprocal-space tight-binding calculations presented here the supercell contains 20 atoms, each from one of the (310) planes parallel to the boundary. There are two grain boundaries in this cell separated by ten (310) planes and the lattice symmetry of the supercell is base-centred orthorhombic. This supercell is shown in figure 2 of Ochs *et al.* (2000) and is reproduced in figure 1 of this paper to make the paper self-contained. A corresponding simple orthorhombic supercell with twice the volume is bounded by (310) and (1 $\bar{3}$ 0) planes in two directions and (001) planes in the third direction.

In order to compare the results of the different approaches consistently, the calculations employing the real-space methods for evaluation of the total energy (FS potentials, BOP and MGPT) were performed using the same supercell approach as the reciprocal-space calculations. At the same time analogous calculations were made using the effectively infinite blocks described above but the results turned out to be almost the same. Therefore, in tables 1 and 2 and figures 2–5, shown later, only the supercell results are reported. The lateral displacement curves displayed in figures 2, 4 and 5 are symmetrical with respect to positive and negative displacement directions (cf. figures 7 and 8 in the paper by Ochs *et al.* (2000)). The results of the different methods are compared for various distinct steps in the procedure for the structural optimization of the $\Sigma = 5$ STGB and the determination of the geometric translation state. They have been outlined in detail by Ochs *et al.* (2000) and are described in the following sections. The starting point is the ideal, geometrically constructed grain boundary formed by joining two grains in the coincidence configuration shown in figure 1. This configuration is denoted (1) as in the work of Ochs *et al.* (2000). Its supercell has a volume of $10a_0^3$, where a_0 is the zero-pressure equilibrium cubic lattice parameter.

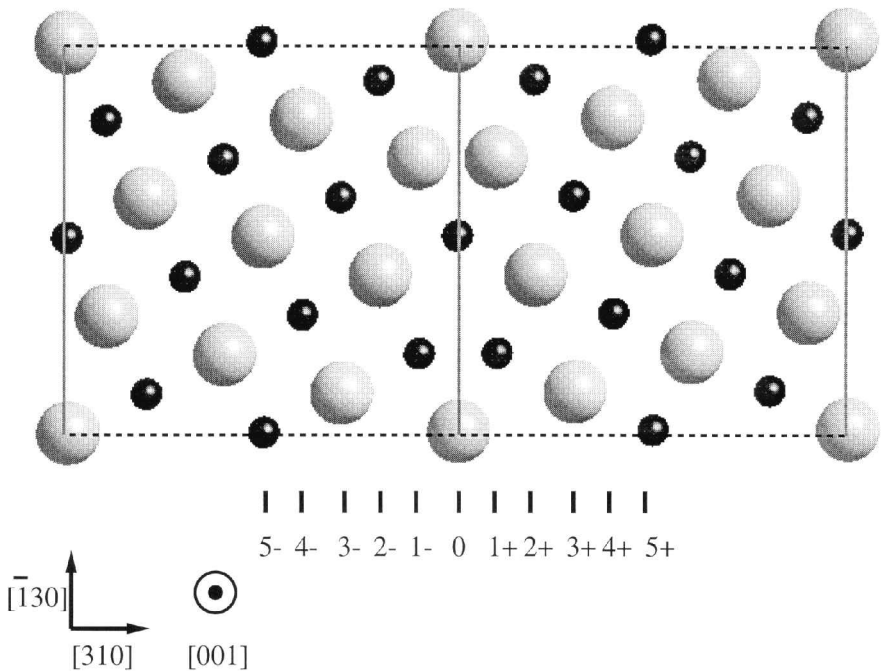
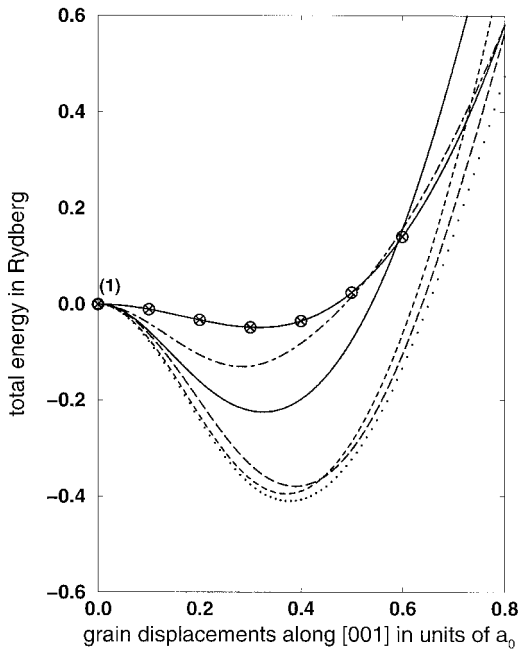


Figure 1. (001) projection of the base-centred orthorhombic supercell containing two mis-oriented bcc grains ((310) slabs) for the $\Sigma = 5$ STGBs. The large grey spheres denote the 20 atoms in the supercell (with periodic boundary conditions) at the ideal positions without any structural optimization; the small black spheres show the atomic positions in adjacent supercells. The 11 symmetry-independent atoms in the supercell ((310) atom layers) are indicated by the numbers 5- to 5+. (Reproduced from figure 2 of Ochs *et al.*(2000).)

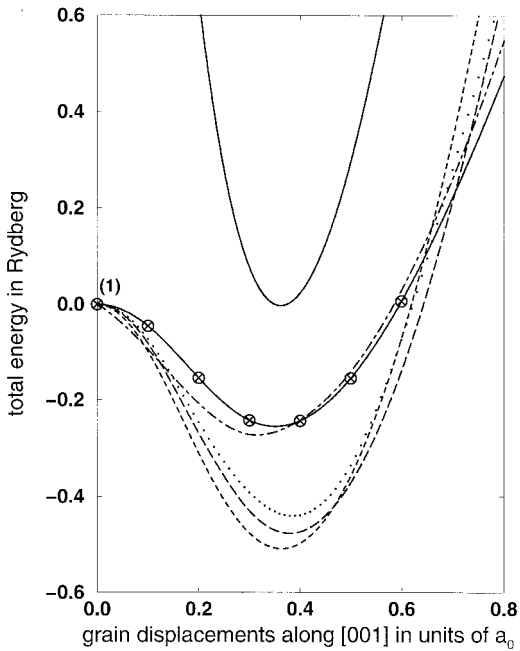
§ 4. COMPARISON OF THE DIFFERENT METHODS WITH RESPECT TO THE STEPWISE STRUCTURAL OPTIMIZATION

4.1. *Relative rigid-body displacements parallel to [001]*

In this first optimization step the two grains are gradually displaced with respect to each other along the [001] direction (the tilt axis) away from configuration (1). During this process all atoms in each block are kept at the corresponding ideal bcc lattice sites, that is no local atomic relaxation is allowed. The dependence of the energy of the supercell on the displacement along [001], calculated by all methods, is shown in figures 2(a) and (b) for Nb and Mo respectively. This displacement results in a lowering of the grain-boundary energy for Nb as well as Mo, yielding a double-well structure of the energy versus displacement curves. Qualitatively the shapes of these curves obtained by LDFT calculations and the five approximate methods, FS, BOP, d-TB, spd-OTB and MGPT, are similar. However, quantitatively the depths of the double wells obtained with different methods vary. In fact, for all cases but the MGPT of Mo the energy is measured relative to the unrelaxed configuration (1). In the latter case the energy associated with configuration (1) is very high owing to a significantly more repulsive interaction and for this reason the energy is referred relative to the displaced minimum-energy configuration. This demonstrates that



(a)



(b)

Figure 2. Total energy versus lateral rigid-grain displacement along [001], starting from configuration (1) (initial geometrical STGB model; cf. figure 1) without relaxation of the atomic positions for (a) Nb and (b) Mo. The data from the different methods are indicated as follows: (— \otimes —), LDFT; (---), d-TB; (-·-·-), spd-OTB; (·····), BOP; (·····), FS; (——), MGPT.

despite a stronger short-range repulsion for the MGPT than in the other methods, the energy dependence on the [001] displacement has qualitatively the same shape.

The LDFT calculations suggest a significant difference between Nb and Mo. The well is much shallower in the former case, signalling the important difference between the relative displacements of the grains found in fully relaxed structures (§ 4.3) and HRTEM observations. This trend is well reproduced by BOPs while the other four methods qualitatively do not differentiate between Nb and Mo at this stage. Quantitatively, MGPT yields a clear difference between the two metals. As seen below, d-TB, spd-OTB and MGPT also differentiate correctly between Nb and Mo in more relaxed structures and only the FS method is unable to reproduce the difference. Thus it is unlikely that the attractive part of the energy in the d-TB, spd-OTB and MGPT methods is responsible for the behaviour found at this stage. The reason most probably lies in the repulsive part. Indeed, during the displacement considered here some atoms come significantly more closely together than the separation of the nearest neighbours in the bcc lattice and thus the short-range repulsion may dominate. The same applies, of course, in the case of BOPs. Therefore, at this stage the results just suggest that the repulsive part of the energy has been fitted better for the BOPs than for the other methods. This is, presumably, because *ab-initio* calculated energy differences for the same atomic volume between bcc and structures with a reduced separation of atoms, such as sc were reproduced when constructing the repulsive terms of the energy.

4.2. *Mirror-symmetry-preserving optimization of the grain-boundary expansion*

In the second optimization step, the grain-boundary structure (1) is relaxed under the constraint that the mirror symmetry with respect to the grain-boundary plane is preserved. This optimization path corresponds to gradually increasing relative displacement of the grains along the [310] direction followed by relaxation of all atomic positions in the supercell under the constraint of the symmetry preservation. The [310] displacement leads to an expansion and thus to an excess volume at the grain boundary. For this reason this calculation was carried out using all methods except the MGPT for Nb for which the potential is available for the equilibrium density only. This path corresponds to the path (2)–(4) in figure 5 of Ochs *et al.* (1999). The present results of the empirical techniques are displayed together with the LDFT results from Ochs *et al.* (2000) in figures 3(a) and (b) for Nb and Mo respectively. The minima of all displayed curves (the LDFT values are denoted by (4)) indicate the structurally optimized grain-boundary configurations with conserved mirror symmetry. Qualitatively the expansions found by various methods and by the LDFT calculations are similar.

Quantitatively the expansions and related energy gains are generally larger for the semiempirical models. This difference can again be attributed to the short-range repulsion. In the present case such repulsion is dominant between the atoms in layers +1 and -1 in the grain-boundary supercell (see figure 1). This is the reason why the optimization step corresponding to the path (1)–(3) in figure 5 of Ochs *et al.* (2000), that is rigid grain displacements along [310] without relaxation of atomic positions, has been omitted in this paper. This step would be completely dominated by the above-mentioned short-range repulsion.

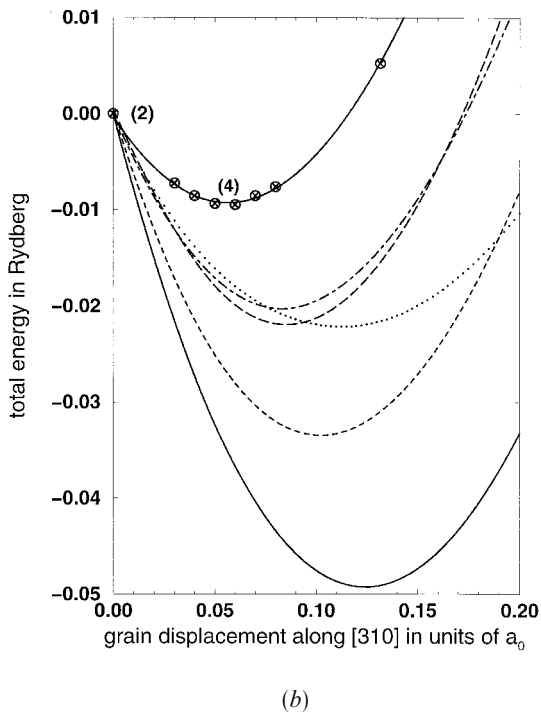
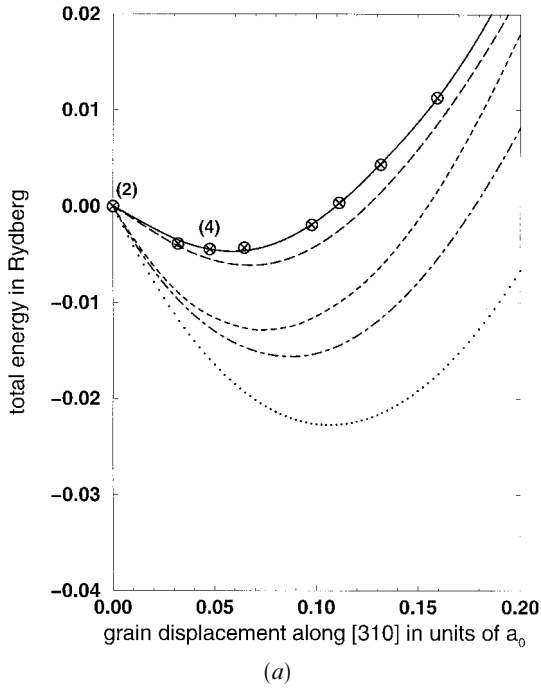


Figure 3. Total energy versus mirror-symmetry-conserving axial grain displacement along [001] (configurations (2) \rightarrow (4)) for (a) Nb and (b) Mo (cf. table 2 and figure 5 of Ochs *et al.* (2000)). The meanings of the symbols are the same as in figure 2.

4.3. Optimization breaking the mirror symmetry

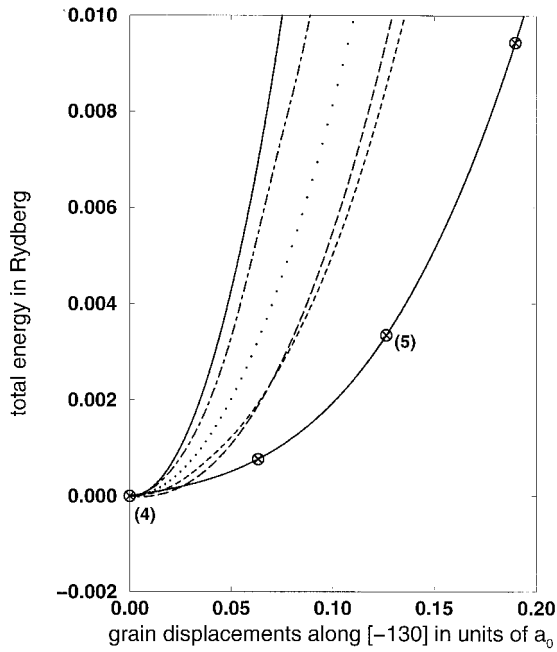
The optimization steps discussed in this section probe for all methods but the MGPT for Nb the stability of the grain-boundary configurations with conserved mirror symmetry, denoted (4) in the previous section. In the case of MGPT for Nb the corresponding mirror-symmetry-conserving configuration has been obtained from configuration (1) by relaxing all atomic positions under the constraint of the symmetry preservation and constant overall density, thus yielding configuration (2). Hence, in the following for the MGPT for Nb, (4) corresponds to this boundary configuration (2). First, the breaking of the mirror symmetry is accomplished by mutually displacing the grains in directions perpendicular ($[\bar{1}30]$) and parallel ($[001]$) to the tilt axis respectively, while keeping the positions of individual atoms in each grain fixed. The former path corresponds to that denoted (4) \rightarrow (5) in table 2 and figure 5 of Ochs *et al.* (2000) and the latter to (4) \rightarrow (6). The second step involves complete structural optimization, allowing for both the relative displacement of the grains in any direction and the relaxation of positions of individual atoms.

Figures 4(a) and (b) display the dependence of the total energy on the displacement in the $[\bar{1}30]$ direction for Nb and Mo respectively. Qualitatively all semiempirical models, in accordance with LDFT, demonstrate that configuration (4) is stable with respect to such displacement. For Mo the results of all models coincide very closely. However, for Nb the variation is larger. For example, the FS method predicts for Nb almost the same energy increase with the $[\bar{1}30]$ displacement as for Mo but LDFT indicates a considerably weaker increase. The results of the spd-OTB and d-TB models fall between those of the FS and LDFT methods but for BOPs the energy increases with increasing displacement appreciably more strongly. These quantitative differences can again be attributed to differences in the parametrized short-range repulsion in the semiempirical models.

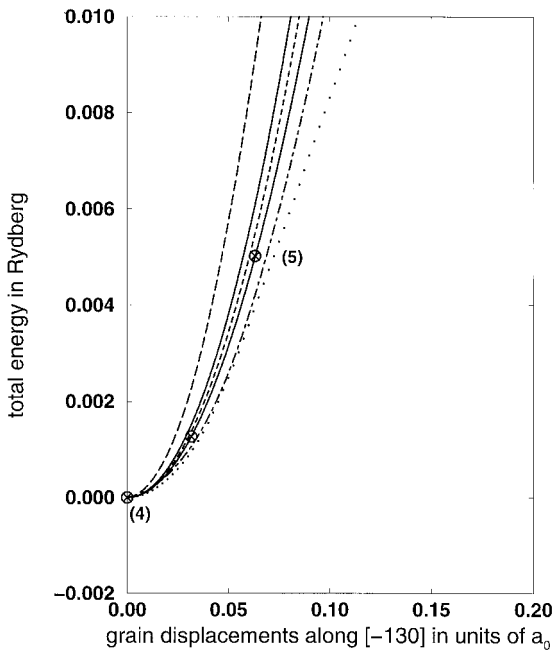
The dependences of the total energy on the displacement in the $[001]$ direction are shown in figures 5(a) and (b) for Nb and Mo respectively. This relaxation step turns out to be the most interesting, since the models considered here do not all lead to qualitatively the same stable configurations. In Mo, configuration (4) is found to be unstable by all the methods used. The minimum-energy configuration (denoted (6) for LDFT) possesses a displacement along $[001]$ and thus a broken mirror symmetry. However, the magnitude of this displacement and the related decrease in the energy relative to configuration (4) varies. Both are the largest for BOPs and MGPT, and smallest for the d-TB method; the spd-OTB and FS models are in between but close to LDFT. These variations are again related to differences in the parametrized short-range repulsion.

However, the situation is different in Nb. The FS method again leads to a slight metastability of configuration (4) and to a configuration with broken mirror symmetry although the energy decrease relative to configuration (4) is smaller than in Mo. In contrast, all the other semiempirical methods predict that configuration (4) is stable with respect to $[001]$ displacements of the grains. The LDFT results lie in between; the minimum-energy configuration (6) corresponds to a small displacement, $0.06a_0$, with a supercell total-energy decrease of $0.1 \text{ mRyd} = k_B \times 16 \text{ K}$ (k_B is the Boltzmann constant) relative to configuration (4). For all practical purposes this configuration is indistinguishable from that with no displacement (cf. Ochs *et al.* (2000)).

Finally, the full optimization of both the relative displacements of the grains and positions of individual atoms leads to distinctly different configurations in Nb and



(a)



(b)

Figure 4. Total energy versus mirror-symmetry-breaking lateral grain displacement along $[\bar{1}30]$ (configurations (4) \rightarrow (5)) for (a) Nb and (b) Mo (cf. table 2 and figures 7 (b) and 8 (b) of Ochs *et al.* (2000)). The meanings of the symbols are the same as in figure 2.

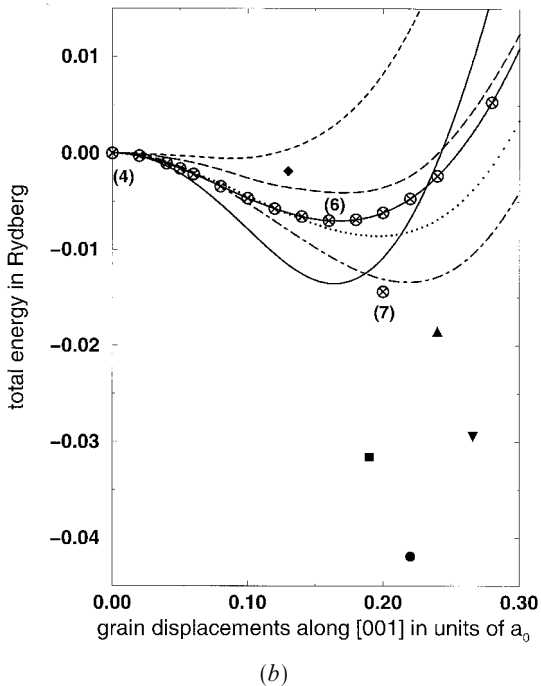
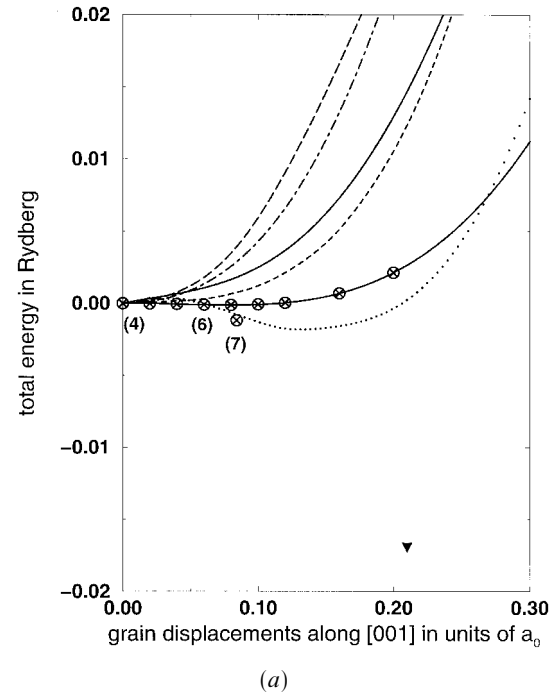


Figure 5. Total energy versus mirror-symmetry-breaking lateral grain displacement along [001] (configurations (4) \rightarrow (6) and (7)) for (a) Nb and (b) Mo (cf. table 2 and figures 7 (b) and 8 (b) of Ochs *et al.* (2000)). The meanings of the symbols are the same as in figure 2. Additionally, the following symbols are used to mark configurations (7): (\blacklozenge), d-TB; (\blacktriangle), spd-OTB; (\bullet), BOP; (\blacktriangledown), FS; (\blacksquare), MGPT.

Mo, denoted (7) for LDFT in figures 5(a) and (b), for all the methods but FS potentials. The latter method yields very similar configurations with broken mirror symmetry and substantially lower energy than configuration (4), in both Nb and Mo. On the other hand, all the other semiempirical methods give the mirror symmetric configuration (4) as the lowest-energy structure in Nb and predict that in Mo the lowest-energy structure does not possess the mirror symmetry. In the latter case the same has also been found using LDFT. Furthermore, for Mo LDFT, the spd-OTB, BOP and MGPT models all lead to very similar [001] displacements of the grains (about $0.2a_0$) although the energy decrease relative to configuration (4) varies (see figure 5(b)). The d-TB method also predicts a broken mirror symmetry but both the [001] displacement and the associated energy decrease are only marginal. Similarly, the displaced configuration was also found in earlier calculations of Marinopoulos *et al.* (1995) who employed a 4MTB potential.

However, LDFT results differ somewhat from those of the semiempirical methods in the case of Nb (for more details see Ochs *et al.* (2000)). Configuration (7) corresponds to a small [001] displacement by $0.08a_0$ and thus a marginally broken mirror symmetry. At the same time the supercell total-energy decrease of $1.2 \text{ mRyd} = k_B \times 189 \text{ K}$ with respect to configuration (4) is still extremely small. Thus, experimentally it would be very difficult to distinguish between the two configurations. Hence, both the LDFT result and results of all the semiempirical methods but the FS model are compatible with the mirror-symmetry-conserved configuration observed in Nb by HRTEM (Campbell *et al.* 1992, 1993).

§ 5. CONCLUSIONS

The numerical data obtained with the six different theoretical total-energy schemes for grain-boundary energies and relative grain displacements of the optimized STGB translation states, with (4) or without (7) conserved mirror symmetry, are collected in tables 1 and 2 for Nb and Mo respectively. The results of earlier calculations of Campbell *et al.* (1993) for Nb and of Marinopoulos *et al.* (1995) for Mo are also included for comparison. Additionally, to support the fact that the employed 20-atom supercell is sufficiently large for investigations of the $\Sigma = 5$ STGB, new LDFT and spd-OTB data for E_{GB} , obtained since the submission of the paper by Ochs *et al.* (2000) using a 40-atom supercell with the grain-boundary planes being separated twice as far, are given in parentheses in tables 1 and 2. Most models consistently predict preferred STGB translation states with fully or nearly conserved mirror symmetry for Nb and with broken mirror symmetry for Mo, in accordance with the results of HRTEM bicrystal experiments (Campbell *et al.* 1992, 1993, 1999). The two exceptional cases are the FS method, which yields a distinct symmetry breaking configuration (7) with lowest energy for Nb, and the d-TB method, in which the symmetry breaking configuration (7) is energetically nearly degenerate with the symmetric configuration (4) for Mo. Both these cases are in conflict with the HRTEM observations.

Furthermore, with the FS potentials for both Nb and Mo, additional, locally metastable configurations were found to originate from structural instabilities of the configurations (4) with respect to grain displacements along $[\bar{1}30]$ directions. In none of the other schemes was an indication of such an instability observed. However, a very similar behaviour was found in the EAM calculations of Campbell *et al.* (1993) for Nb. The appearance of such additional metastable configurations already in very simple grain boundaries such as the $\Sigma = 5$ STGB indicates that quantitative predic-

Table 1. Optimized macroscopic translation states for the $\Sigma = 5$ STGB in Nb calculated with the different methods: symmetries, grain-boundary energies E_{GB} , magnitudes of the macroscopic grain translations in percentages of the equilibrium lattice constants a_0 . For comparison the results of Campbell *et al.* (1993) for Nb obtained with an EAM potential are included.

Mirror symmetry configuration	E_{GB} (mJm ⁻²)	Grain displacement along the direction		
		[310]	$\bar{[130]}$	[001]
LDFT (Ochs <i>et al.</i> 2000)				
Yes, (4)	1296 (1284)	5	0	0
No, (7)	1288 (1277)	5	0	8
spd-OTB				
Yes, (4) = (7)	1070 (1016)	6	0	0
d-TB				
Yes, (4) = (7)	1585	8	0	0
BOP				
Yes, (4) = (7)	1396	9	0	0
FS				
Yes, (4)	1227	11	0	0
No, (7)	1120	11	0	21
No	1066	6	17	25
MGPT				
Yes, (2)	1159	—	0	0
EAM (Campbell <i>et al.</i> 1993)				
Yes, (4)	1200	—	0	0
No, (7)	1030	—	0	25
No	980	—	16	25

tions of grain-boundary structures in bcc metals obtained with FS or EAM potentials should be considered *a priori* with caution and carefully tested against more accurate approaches.

In general, the empirical schemes, which account for the directional bonding arising from the partially filled d band, all lead to similar results and compare well with the results of non-empirical LDFT. The simplest of these methods, the d-TB model, turns out to be rather good for Nb. For Mo it has the weakness of predicting an almost mirror-symmetrical equilibrium STGB configuration but owing to its simplicity it could be improved without much effort. Considering all the results listed in the tables 1 and 2, for both metals the grain-boundary energies and grain displacements obtained using the spd-OTB model follow most closely those found by the LDFT calculations. Hence, in the context of the present study this method appears to be most accurate of the semiempirical schemes considered. However, it is also the most elaborate and at present limited to reciprocal-space calculations. Both the BOP and the MGPT schemes reproduce correctly all the qualitative features of LDFT calculations, such as positions of the shapes on energy versus displacement curves and relative displacements of the grains, but quantitatively the calculated values of energy differences are less reliable. As discussed in this paper the main reason is not the inaccurate evaluation of the attractive, band or bond

Table 2. Optimized macroscopic translation states for the $\Sigma = 5$ STGB in Mo calculated with the different methods: symmetries, grain-boundary energies E_{GB} , magnitudes of the macroscopic grain translations in percentages of the equilibrium lattice constants a_0 . For comparison the results of Campbell *et al.* (1995) for Mo obtained with a semiempirical 4MTB potential are included.

Mirror symmetry configuration	E_{GB} (mJ m ⁻²)	Grain displacement along the direction		
		[310]	[$\bar{1}$ 30]	[001]
LDFT (Ochs <i>et al.</i> 2000)				
Yes, (4)	1808 (1826)	6	0	0
No, (7)	1702 (1711)	6	0	20
spd-OTB				
Yes, (4)	1563 (1479)	8	0	0
No, (7)	1432 (1370)	8	0	24
d-TB				
Yes, (4)	1784	10	0	0
No, (7)	1772	10	0	13
BOP				
Yes, (4)	1365		0	0
No, (7)	1274	8	0	22
FS				
Yes, (4)	1535	11	0	0
No	1532	11	2	0
No, (7)	1300	11	0	26
MGPT				
Yes, (4)	2124	12	0	0
No, (4)	1904	11	0	19
4MTB (Marinopoulos <i>et al.</i> 1995)				
Yes, (4)	2032	9	0	0
No, (7)	1918	10	0	17

energy but an inaccurate description of repulsive interactions for atomic separations smaller than the first-nearest neighbour spacings. However, this effect is more significant in unrelaxed structures than in fully relaxed, physically significant structures since, in the latter case, atomic separations smaller than the nearest-neighbour spacing is not common. The former is seen, for example, in figure 5 (b) which shows that the relative decrease of the energy due to full relaxation is significantly larger for the BOP, MGPT and FS methods than for the LDFT and spd-OTB methods. However, table 2 shows that the energies of the relaxed structures are very similar for all the schemes considered.

In summary, the comparative study of five semiempirical total energy schemes with a non-empirical LDFT calculation demonstrates that the real-space (BOP and MGPT) and reciprocal-space (d-TB and spd-OTB) models that all extend beyond the second-moment approximation to the density of states are suitable for studies of grain boundaries and, most probably, for other extended defects in bcc transition metals. The FS method based on the second-moment approximation must be treated with care when applied in such studies since any directional bonding due to d electrons is neglected.

ACKNOWLEDGEMENTS

The authors gratefully acknowledge collaborations and fruitful discussions concerning the developments of the spd-OTB model with H. Haas, of the d-TB model with A. T. Paxton and of the bond-order potentials with D. Nguyen-Manh and D. G. Pettifor. This work was supported in part by the Advanced Strategic Computing Initiative of the US Department of Energy through Lawrence Livermore National Laboratory grant B331542 (M.M. and V.V.), and by the US Department of Energy, contract W-7405-ENG-48 (J.B. and J.A.M.). V.V. would like to acknowledge support by the Humboldt Foundation during his stay at the Max-Planck-Institut für Metallforschung Stuttgart.

REFERENCES

- ACKLAND, G. J., 1992, *Phil. Mag. A*, **66**, 917.
 ACKLAND, G. J., FINNIS, M. W., and VITEK, V., 1988, *J. Phys. F*, **18**, L153.
 ACKLAND, G. J., and THETFORD R., 1987, *Phil. Mag. A*, **56**, 15.
 ACKLAND, G. J., TICHY, G., VITEK, V., and FINNIS, M. W., 1987, *Phil. Mag. A*, **56**, 735.
 ACKLAND, G. J., and VITEK, V., 1990, *Phys. Rev. B*, **41**, 10324.
 AOKI, M., 1993, *Phys. Rev. Lett.*, **71**, 3842.
 BACIA, M., MORILLO, J., PÉNISSON, J. M., and PONTIKIS, V., 1997, *Phil. Mag. A*, **76**, 945.
 BOWLER, D. R., AOKI, M., GORINGE, C. M., HORSFIELD, A. P., and PETTIFOR, D. G., 1997, *Modelling Simulation Mater. Sci. Engng.*, **5**, 199.
 BROUGHTON, J., BRISTOWE, P., and NEWSAM, J. (editors), 1993, *Materials Theory and Modelling*, Materials Research Society Symposium Proceedings, Vol. 291 (Pittsburgh, Pennsylvania: Materials Research Society).
 CAMPBELL, G. H., BELAK, J., and MORIARTY, J. A., 1999, *Acta mater.*, **47**, 3977.
 CAMPBELL, G. H., FOILES, S. M., GUMBSCH, P., RÜHLE, M., and KING, W. E., 1993, *Phys. Rev. Lett.*, **70**, 449.
 CAMPBELL, G. H., KING, W. E., FOILES, S. M., GUMBSCH, P., and RÜHLE, M., 1992, *Structure and Properties of Interfaces in Materials*, Materials Research Society Symposium Proceedings, Vol. 238, edited by W. A. T. Clark, U. Dahmen and C. L. Briant (Pittsburgh, Pennsylvania: Materials Research Society), p. 163.
 CARLSSON, A. E., 1991, *Phys. Rev. B*, **44**, 6590.
 DAW, M. S., and BASKES, M. I., 1984, *Phys. Rev. B*, **29**, 6443.
 DAW, M. S., FOILES, S. M., and BASKES, M. I., 1993, *Mater. Sci. Rep.*, **9**, 251.
 ELSÄSSER, C., BECK, O., OCHS, T., and MEYER, B., 1998, *Microscopic Simulation of Interfacial Phenomena in Solids and Liquids*, Materials Research Society Symposium Proceedings, Vol. 492, edited by S. R. Phillpot, P. D. Bristowe, D. R. Stroud and J. R. Smith (Pittsburgh, Pennsylvania: Materials Research Society), p. 121.
 ELSÄSSER, C., TAKEUCHI, N., HO, K.-M., CHAN, C. T., BRAUN, P., and FÄHNLE, M., 1990, *J. Phys.: condens. Matter*, **2**, 4371.
 FINNIS, M. W., and SINCLAIR, J. E., 1984, *Phil. Mag. A*, **50**, 45; 1986, *ibid.*, **53**, 161.
 FOILES, S. M., 1993, *Phys. Rev. B*, **48**, 4287; 1996, *Mater. Res. Soc. Bull.*, **21**(2), 24.
 FRIEDEL, J., 1969, *The Physics of Metals*, edited by J. M. Ziman (Cambridge University Press), p. 340.
 FU, C.-L., and HO, K.-M., 1983, *Phys. Rev. B*, **28**, 5480.
 GIRSHICK, A., BRATKOVSKY, A. M., PETTIFOR, D. G., and VITEK, V., 1998a, *Phil. Mag. A*, **77**, 981.
 GIRSHICK, A., PETTIFOR, D. G., and VITEK, V., 1998b, *Phil. Mag. A*, **77**, 999.
 HAAS, H., WANG, C. Z., FÄHNLE, M., ELSÄSSER, C., and HO, K. M., 1998a, *Phys. Rev. B*, **57**, 1461; 1998b, *Tight-Binding Approach to Computational Materials Science*, Materials Research Society Symposium Proceedings, Vol. 491, edited by P. E. A. Turchi, A. Gonis and L. Colombo (Pittsburgh, Pennsylvania: Materials Research Society), p. 327.
 HARRISON, W. A., 1980, *Electronic Structure and the Properties of Solids* (San Francisco, California: Freeman); 1994, *Surf. Sci.*, **30**, 298.

- HO, K. M., ELSÄSSER, C., CHAN, C. T., and FÄHNLE, M., 1992, *J. Phys.: condens. Matter*, **4**, 5189.
- HOHENBERG, P., and KOHN W., 1964, *Phys. Rev.*, **136**, B864.
- HORSFIELD, A. P., BOWLER, D. R., GORINGE, C. M., PETTIFOR, D. G., and AOKI, M., 1998, *Tight-Binding Approach to Computational Materials Science*, Materials Research Society Symposium Proceedings, Vol. 491, edited by P. E. A. Turchi, A. Gonis and L. Colombo (Pittsburgh, Pennsylvania: Materials Research Society), p. 417.
- HORSFIELD, A. P., BRATKOVSKY, A. M., FEARN, M., PETTIFOR, D. G., and AOKI, M., 1996a, *Phys. Rev. B*, **53**, 12694.
- HORSFIELD, A. P., BRATKOVSKY, A. M., PETTIFOR, D. G., and AOKI, M., 1996b, *Phys. Rev. B*, **53**, 1656.
- KOHN, W., and SHAM, L. J., 1965, *Phys. Rev.*, **140**, A1133.
- LEGRAND, B., 1984, *Phil. Mag. A*, **52**, 83.
- LOUIE, S. G., HO, K.-M., and COHEN, M. L., 1979, *Phys. Rev. B*, **19**, 1774.
- LUDWIG, M., and GUMBSCH, P., 1995, *Modelling Simulation Mater. Sci. Engng.*, **3**, 533.
- MARINOPOULOS, A. G., VITEK, V., and CARLSSON, A. G., 1995, *Phil. Mag. A*, **72**, 1311.
- MARK, J. E., GLICKSMAN, M. E., and MARSH, S. P. (editors) 1992, *Computational Methods in Materials Science*, Materials Research Society Symposium Proceedings, Vol. 278 (Pittsburgh, Pennsylvania: Materials Research Society).
- MEYER, B., ELSÄSSER, C., and FÄHNLE, M., 1998, Fortran90 Program for Mixed-Basis Pseudopotential Calculations for Crystals, Max-Planck-Institut für Metallforschung Stuttgart.
- MORIARTY, J. A., 1988, *Phys. Rev. B*, **38**, 6941; 1990, *ibid.*, **42**, 1609; 1994, *ibid.*, **49**, 12431.
- MROVEC, M., VITEK, V., NGUYEN-MANH, D., PETTIFOR, D. G., WANG, L. G., and SOB, M., 1999, *Multiscale Modeling of Materials*, Materials Research Society Symposium Proceedings, Vol. 538, edited by V. Bulatov, N. Ghoniem, T. Diaz de la Rubia and T. Kaxiras (Pittsburgh, Pennsylvania: Materials Research Society), p. 529; 2000 (to be published).
- NGUYEN-MANH, D., PETTIFOR, D. G., ZNAM, S., and VITEK, V., 1998, *Tight-Binding Approach to Computational Materials Science*, Materials Research Society Symposium Proceedings, Vol. 491, edited by P. E. A. Turchi, A. Gonis and L. Colombo (Pittsburgh, Pennsylvania: Materials Research Society), p. 353.
- OCHS, T., BECK, O., ELSÄSSER, C., and MEYER, B., 2000, *Phil. Mag. A*, **80**, 351.
- PAXTON, A. T., 1996, *J. Phys. D*, **29**, 1689.
- PETTIFOR, D. G., 1989, *Phys. Rev. Lett.*, **63**, 2480; 1995, *Bonding and Structure of Molecules and Solids* (Oxford University Press).
- PETTIFOR, D. G., and WEAIRE, D. L., 1985, *Solid St. Phys.*, **58**.
- PHILLPOT, S. R., BRISTOWE, P. D., STROUD, D. R., and SMITH, J. R. (editors), 1998, *Microscopic Simulation of Interfacial Phenomena in Solids and Liquids*, Materials Research Society Symposium Proceedings, Vol. 492 (Pittsburgh, Pennsylvania: Materials Research Society).
- SLATER, J. C., and KOSTER, G. F., 1954, *Phys. Rev.*, **94**, 1498.
- SPANJAARD, D., and DESJONQUERES, M. C., 1984, *Phys. Rev. B*, **30**, 4822.
- SUTTON, A. P., and BALLUFFI, R. W., 1995, *Interfaces in Crystalline Materials* (Oxford: Clarendon).
- SUTTON, A. P., FINNIS, M. W., PETTIFOR, D. G., and OHTA, Y., 1988, *J. Phys. C*, **21**, 35.
- TURCHI, P. E. A., GONIS, A., and COLOMBO, L., 1998, *Tight-Binding Approach to Computational Materials Science*, Materials Research Society Symposium Proceedings, Vol. 491 (Pittsburgh, Pennsylvania: Materials Research Society).
- VITEK, V., 1994, *The Encyclopedia of Advanced Materials*, edited by D. Bloor, R. J. Brook, M. C. Flemings and S. Mahajan (Oxford: Pergamon), p. 153; 1996, *Stability of Materials*, NATO Advanced Study Institute Series, edited by A. Gonis P. E. A. Turchi and J. Kudrnovsky (New York: Plenum), p. 53.
- VOTER, A. F. (editor), 1996, *Mater. Res. Soc. Bull.*, **21**(2), 17.
- XU, W., and MORIARTY, J. A., 1996, *Phys. Rev. B*, **54**, 6941; 1998, *Comput. Mater. Sci.*, **9**, 348.
- YAN, M., VITEK, V., and CHEN, S. P., 1996, *Acta Mater.*, **44**, 4351.